Texture Orientation Modulation for Halftoning Watermarking

Jing-Ming Guo, *Senior Member, IEEE*, Chang-Cheng Su, and Yun-Fu Liu, *Student Member, IEEE*

Department of Electrical Engineering,
National Taiwan University of Science and Technology
Taipei, Taiwan
E-mail: jmguo@seed.net.tw, changchengsu@gmail.com, yunfuliu@gmail.com

ABSTRACT

In this paper, a halftoning-based watermarking scheme with high data capacity and image quality is presented. Three types of watermarks of various pixel-depths, including 1-bit, 2-bit, and 3-bit, are able to be embedded without prominently damaging the image quality. To achieve high marked image quality, the parallel-oriented high efficient Direct Binary Search (DBS) halftoning is adopted to cooperate with the proposed Orientation Modulation (OM) method. In the decoder, the Least-Mean-Square-trained (LMS-trained) filters are adopted to extract the features of marked images in the frequency domain, and the naïve Bayes classifier is employed to analyze the extracted features and further decode the watermark information. Experimental results demonstrate that the proposed DBS-based OM encoding scheme provides excellent image quality, high processing efficiency, and high robustness to adapt to practical printing application.

***Key words:** Halftoning, LMS, halftone image classification, naïve Bayes classifier.*

1. INTRODUCTION

Digital halftoning [1] is a technique to display grayscale images in two-tone binary, these halftone images can be misinterpreted as continue-tone images when viewing from a distance by the low-pass nature of the Human Visual System (HVS). Many different halftoning methods have been developed, including Direct Binary Search (DBS) [2]-[4], Ordered Dithering (OD) [5], Error Diffusion (ED) [6], Dot Diffusion (DD) [7]. Among these, DBS offers the best image quality, however it also gears with the highest computational complexity.

Digital watermarking has many applications, the type of watermarking can be separated into two categories according to the visibility of the watermark embedded in a marked image. In this paper, a watermarking for halftone images, namely DBS-based Orientation Modulation (OM), belonging to the invisible category. The proposed scheme adopts the concept of the DBS halftoning and the features of various texture angles to embed a watermark. Moreover, the Least-Mean-Square (LMS) algorithm and the naïve Bayes classifier are catered for decoding the watermark. According to the experiment results, good image quality, excellent Correct Decode Rate (CDR), and high robustness can be achieved simultaneously. Moreover, due to the fact that the parallel high speed DBS is used, the processing speed is promising.

The rest of this paper is organized as follows. Section 2 provides the definitions of quality assessment methods for a marked image and a decoded watermark. Sections 3 and 4 introduce the proposed DBS-based OM encoder and decoder with the LMS-trained filter and naïve Bayes classifier. The experimental results are given in Section 5, and Section 6 draws conclusions.

2. PERFORMANCE EVALUATIONS

The Human-visual-system Peak Single-to-Noise Ratio (HPSNR) is employed in this study for image quality estimation. This criterion is different from the traditional PSNR which does not consider the nature of HVS. Suppose a test halftone image of size PxQ is estimated, the HPSNR metric is defined as

$$\text{HPSNR} = 10\log_{10}(\frac{P \times Q \times 255^2}{\sum_{i=1}^{P}\sum_{j=1}^{Q}[\sum_{m,n \in R}\sum q_{m,n}(g_{i+m,j+n} - h_{i+m,j+n})]^2}), \quad (1)$$

where the variables $g_{i,j}$ and $h_{i,j}$ represent the pixel values of an original grayscale image and its corresponding halftone image, respectively; the value 255 denotes the maximum value of an 8-bit digital image; variable $q_{m,n}$ denotes the coefficient of a 2-D Gaussian filter, where the support region (R) size is set at 7x7. The exact $q_{m,n}$ is derived as below,

$$q_{m,n} = e^{-\frac{1}{2}(\frac{m^2}{\sigma_x^2}+\frac{n^2}{\sigma_y^2})}, \quad (2)$$

where the variables σ_x and σ_y denote the standard deviations along the two perpendicular directions. In this study, the summation of the derived Gaussian coefficients is normalized to 1 before it is used. The two parameters σ_x and σ_y are both set at 1.3.

The quality of a decoded watermark of size MxN is estimated with the following criterion, namely Correct Decoding Rate (CDR).

$$\text{CDR} = \frac{\sum_{m=1}^{M}\sum_{n=1}^{N}w_{m,n}\Theta dw_{m,n}}{M \times N}\times 100\%, \quad (3)$$

where $w_{m,n}$ and $dw_{m,n}$ denote an original watermark and a decoded watermark, respectively; operator Θ denotes the exclusive NOR (XNOR) operation. Notably, the watermarks used in this study contains various pixel-depths, and thus the "correctly decoding" only occurs when $w_{m,n} = dw_{m,n}$.

3. PROPOSED DIRECT BINARY SEARCH-BASED ORIENTATION MODULATION ENCODING SCHEME

In this section, the proposed DBS-based OM encoding scheme is discussed, the corresponding flowchart is illustrated in Fig. 1(a). First, the grayscale host image of size PxQ is divided into many non-overlapped sub-images of size (P/M)x(Q/N). Each pixel of the watermark of size MxN is embedded into an individual sub-image. In this study, the bit-depth of a watermark can be ranged from 1- to 3-bit. This characteristic can drive the proposed method providing a higher data capacity. Notably, each divided sub-image can be processed simultaneously and offer good parallel property to improve the processing efficiency.

In this study, the improved efficient DBS [3] method is further modified with the Orientation Modulation (OM) to achieve an additional watermarking function. The efficient DBS represents the nature of HVS generated by Nasanen's Contrast Sensitivity Function (CSF) [8] in the spatial domain. The proposed is modified point spread function to represent different watermark values. The CSF used to derived $\tilde{p}(s,t)$ is replaced with the modified 2-D Gaussian distribution which can to easily control to generate halftones with various directions as below,

$$\widetilde{p}(s,t) = e^{-(as^2+\eta bst+ct^2)}, \quad (4)$$

where the parameter η denotes the quality factor which directly affects the image quality as will be discussed later; variables a, b, and c are defined as below,

$$a = \frac{\cos^2\theta}{2\sigma_s^2} + \frac{\sin^2\theta}{2\sigma_t^2}, \quad (5)$$

$$b = -\frac{\sin 2\theta}{4\sigma_s^2} + \frac{\sin 2\theta}{4\sigma_t^2}, \quad (6)$$

$$c = \frac{\sin^2\theta}{2\sigma_s^2} + \frac{\cos^2\theta}{2\sigma_t^2}, \quad (7)$$

where the two empirical parameters σ_s and σ_t denote the standard deviations, and which are set at 1 and 2 respectively to simulate the ellipse distribution shape; variable $\theta \in (0^\circ, 180^\circ)$ denotes the angle,

which is controlled by various embedded watermark values. Notably, the proposed watermarking method can embed watermarks of various pixel-depths, for example, N-bit, where $N=1$ to 3 in this study, and each of them contains 2^N colors. In this study, since each angle represents a specific color, for maximizing the distinguish capability of each halftone texture angle, the difference between each pair of consecutive angles is defined as below,

$$\Delta \theta = \frac{180^\circ}{2^N}, \tag{8}$$

where 2^N denotes the number of representing colors. For an instance, when a watermark of 2-bit pixel-depth (N = 2) is embedded in a halftone image, then each of the four angles 0°, 45°, 90°, and 135° can be used to represent each of the 2^2 watermark colors.

4. PROPOSED DECODING SCHEME WITH THE LEAST-MEAN-SQUARE FILTERS AND THE NAÏVE BAYES CLASSIFIERS

Figure 1(b) illustrates the decoding procedure of a marked sub-image. First, a marked sub-image is transformed into the frequency domain by the Fast Fourier Transform (FFT) for feature extraction using the proposed LMS-trained filters. Subsequently, the naïve Bayes classifier are adopted to extract the watermark information according these extracted features. The details are discussed below.

4.1. Features extraction

Various texture orientations used on each sub-image embedding can yield a slightly different spatial dot distribution density which is not easily perceived by human eye. Yet, it can be obviously observed in the frequency domain. Figure 2 shows some instances, where the pattern on the right hand side of each pair is transformed by the FFT. To distinguish the orientation characteristics, L LMS-trained filters corresponding to L orientations are trained and the procedure as described below,

$$\hat{v}^c = \sum_{m,n \in R} \sum u^k(m,n) \times f_d^c(m,n), \tag{9}$$

$$e^2 = (v - \hat{v}^c)^2, \text{ where } v = \begin{cases} 0, \text{ if } c \neq tc \\ 255, \text{ Otherwise} \end{cases}, \tag{10}$$

$$\frac{\partial e^2}{\partial u^k(m,n)} = -2ef_d^c(m,n), \tag{11}$$

$$u^{k+1}(m,n) = u^k(m,n) + \begin{cases} \gamma ef_d^c(m,n), \text{ if } \frac{\partial e^2}{\partial u^k(m,n)} < 0 \\ -\gamma ef_d^c(m,n), \text{ if } \frac{\partial e^2}{\partial u^k(m,n)} > 0 \end{cases}, \tag{12}$$

where $f_d^c \in \mathbf{F} = \{f_1^c, f_2^c, \cdots, f_D^c\}$ denotes the training halftone patterns in the frequency domain with a fixed size, where the halftone image is generated with a specific angle $c \in \{1,2,\cdots,L\}$, (in total L different angles) and the constant D denotes the number of the training patterns in the frequency domain; variable $u^k(m,n)$ denotes the kth iterated trained filter with a support region R, where the size of R is identical to the size of the pattern training in the frequency domain. The summation of the trained filter is constrained to one to yield an energy convergent result. The $u^k(m,n)$ can be used to distinguish the target class (tc) and the other classes ($\overline{tc}$). In addition, $tc \in c$, and the size is identical to the pattern in the frequency domain. Notably, the target value (v) is determined by whether c is equal to tc. If yes, then $v=255$; otherwise, $v=0$. The target values are set to the theoretical maximum (255) and minimum (0) of a digital image to provide better discrimination results. In this training algorithm, the converge speed (γ) is set at 10^{-10}. The feature is calculated by

$$x_c = \sum_{m,n \in R} \sum u_c(m,n) \times H(m,n), \tag{13}$$

where $H(m,n)$ denotes a marked halftone pattern $h(m,n)$ in the frequency domain, and the variable $u_c(m,n)$ denotes the coefficient of the LMS-trained filter with angle c.

4.2. Naïve Bayes classifier

Figure 3 shows the normalized feature distributions, in which each color line on each subfigure is averaged from 25600 halftone patterns in the frequency domain, and the distribution of each subfigure is obtained by one LMS-trained filter of a specific angle. Based on the observation of these results, two properties can be yielded: 1) the feature values which have the same class of the employed LMS-trained filters are higher than others classes, and 2) except for the class which belongs to the employed LMS-trained filter, other feature distributions also show the possibility for classification. These two observed characteristics are fully utilized to further improve the performance of the correct classification, and the naïve Bayes classifier which is derived from the Bayesian theorem is later proved as a powerful tool to cope with the object as described below:

$$p(H \mid I) = \frac{p(H)p(I \mid H)}{p(I)}, \tag{14}$$

where I denotes information, and H denotes hypothesis. This theorem gives a relationship between the observed information and the future hypothesis. The equation can be rewritten as below for a practical application with number of L information and number of K hypothesizes:

$$p(h_k \mid i_1, i_2, \cdots, i_L) = \frac{p(h_m)p(i_1, i_2, \cdots, i_N \mid h_k)}{p(i_1, i_2, \cdots, i_L)}, \text{ where } 1 \leq k \leq K. \tag{15}$$

The term $p(i_1, i_2, \cdots, i_L \mid h_k)$ can be assumed as independent since it is hard to collect enough information, and which will not affect the performance of the classification significantly [9]. Hence, Eq. (15) can be further rewritten as below:

$$p(h_k \mid i_1, i_2, \cdots, i_L) = \frac{p(h_k) \prod_{b=1}^{L} p(i_b \mid h_k)}{\sum_{a=1}^{K} p(h_a) \prod_{b=1}^{L} p(i_b \mid h_a)}, \tag{16}$$

where the denominator is obtained by the law of total probability. To adapt to the halftoning classification application, and suppose the orientation is divided by four , Eq. (16) is modified as below:

$$p(c_k \mid x_1, x_2, \cdots, x_4) = \frac{p(c_k) \prod_{b=1}^{4} p(x_b \mid c_k)}{\sum_{a=1}^{K} p(c_a) \prod_{b=1}^{4} p(x_b \mid c_a)}, \tag{17}$$

where x_n denotes the feature extracted by the LMS-trained filter of class n, and c_k denotes the orientation k. The probability of $p(c_k)$ is set as uniform since the occurrences of different orientations are assumed with equal probability. The term $p(x_b \mid c_k)$ can be obtained by conducting the feature statistics under the condition when the sub-halftone image is obtained by c_k, and which is shown in Fig. 3.

According to the above derivation, the probabilities of the N angles can be obtained. Subsequently, the Maximum A Posteriori (MAP) rule can be employed for deriving the class with the highest probability. As a result, the final class of a tested halftone image can be determined.

$$\hat{c}_{MAP}(x_1, x_2, \cdots, x_4) = \arg\max_c p(c \mid x_1, x_2, \cdots, x_4), \tag{18}$$

where the term $p(c \mid x_1, x_2, \cdots, x_4)$ is identical to that in Eq. (17). The denominator of $p(c \mid x_1, x_2, \cdots, x_4)$ can be neglected since it is identical to the halftoning scheme. The probability $p(c)$ can be neglected as well since it is uniform. Thus, the MAP can be replaced with the Maximum Likelihood (ML) rule as below:

$$\hat{c}_{ML}(x_1, x_2, \cdots, x_4) = \arg\max_c \prod_{b=1}^{L} p(x_b \mid c), \tag{19}$$

by doing this, the computational complexity can be significantly reduced.

The above decision manner, namely nonparametric decision (NPD), adopts the statistic information consuming a lot of memory for storing the feature distribution. To ease this problem, the parametric decision (PD) method is adopted, and each of the feature distributions is modeled by a 1-D Gaussian distribution with the corresponding mean and standard deviation.

5. EXPERIMENTAL RESULTS

In this section, the performance of the proposed DBS-based OM is

tested with many aspects as below. Figure 4 shows the CDRs of the sub-images of sizes 32x32, where each CDR is averaged from 25 test images of size 512x512, and the watermarks involve three different pixel depths. As introduced in Section 4, in total three different decoders are tested in the experiments:

1) LMS: Due to the calculated features obtained by Eq. (13) directly indicate the similarity with the angle of the LMS-trained filter employed to calculate the feature value, the angle with the maximum feature value is considered as the classified result.

2) Nonparametric decision (NPD): Classify with the naïve Bayes classifier, and the feature distribution is constructed by the statistics such as the results in Fig. 3.

3) Parametric decision (PD): The feature distributions employed by the naïve Bayes classifier are modeled by 1-D Gaussian distributions constructed by the corresponding means and standard deviations of the distributions from the nonparametric statistics.

According to the observation, the quality factor (η) in Eq. (4) is directly proportional to CDR, since this parameter can control the orientation shape of a halftone pattern in the frequency domain. Notably, the circle shape ($\eta=0$) has no direction, and thus η is expected to be greater to provide a better discrimination capability as it can be seen in Fig. 5. Comparing the above three different methods, the nonparametric decision method achieves the best CDR, since it provides more precise analytical capability of the feature distribution than that of the parametric decision. Since the DBS-based OM enjoys the benefit of parallelism, the processing speed is around 422 fps (frame/second) with images of size 512x512. According to the experiments, promising results can be yielded when the sub-image size is set at 32x32, and the parametric decision method is employed, and thus the following experiments are performed with this setting.

Figure 6 shows the relationships among HPSNR, CDR, and quality factor η. Notably, the HPSNR is used to measure the marked halftone image quality. Since the proposed method is able to embed watermarks of various pixel depths, thus three different pixel depths, 1-bit, 2-bit, and 3-bit, are involved. According to the observation, a watermark with a lower pixel depth can yield better performance in terms of HPSNR and CDR. In addition, when the quality factor lower than 0.5, the marked image quality appear saturated, and the CDRs degrade rapidly. Thus, the quality factor is recommended setting at 0.5 in this study. Figure 7 shows some practical marked results and the decoded watermarks. It can be seen that when the pixel depth of an embedded watermark is higher than 2-bit, the CDR cannot maintain 100%. Nonetheless, the decoded results are still promising (around 99% CDR) as shown in Fig. 7(d). Moreover, the enlarged parts as shown on the top-right corner of Fig. 7(b)-(d) indicate that, although the proposed encoder is processed independently, the marked images are not accompanied with blocking effect.

Some distortions, such as cropping and print-and-scan, may be encountered in the practical applications. Figure 8 shows the CDRs under cropping distortion with various cropped sizes, where each data is averaged by 25 different test images, and watermarks of three different pixel depths are also involved in this experiment. Herein, a host image is of size 512x512. Among these, when the cropped sizes are less than or equal to 128, the CDRs can be maintained higher than 90%, thus a higher cropped sizes should be avoided. Figure 9 shows the CDRs of decoded watermarks extracted from the marked images undergone the print-and-scan distortion. Normally, the print-and-scan channel involves zooming, shifting, rotation, and dot gain darkening effect, and which cause severe distortions. It can be seen that the resolution of printing/scanning is inversely/directly proportional to the CDR. According to the experiments, the proposed method is sufficiently robust to be applied on practical applications.

Table I shows the comparisons among the former related methods and the proposed method, where the notations + and − represent advantage and shortcoming, respectively. In this comparison, the proposed method can provide excellent advantages in terms of image quality, robustness, processing efficiency, and data capacity, and thus prove that the proposed method can present excellent performance to address practical halftoning security issues.

6. CONCLUSIONS

This paper presents the DBS-based OM method to hide multi-bit watermarks into halftone images. The DBS is a halftoning scheme which can generate the best halftone patterns, while the processing speed is its deficiency. The DBS-based OM has the parallelism property, and thus which can gear with high quality and processing speed simultaneously. To decode an embedded watermark, the LMS-trained filters and the naïve Bayes classifier are catered to achieve good decoding rates. Moreover, the proposed parametric decision strategy can significantly reduce the memory consumption while yield promising decoded results. As documented in the experimental results, the proposed method provides excellent image quality, high processing efficiency, high embedding capacity, and sufficient robustness to guard against distortions induced from the cropping and print-and-scan which frequently happened in halftone printing.

REFERENCES

[1] R. Ulichney, *Digital Halftoning*. Cambridge, MA: MIT Press, 1987.

[2] M. Analoui and J. P. Allebach, "Model based halftoning using direct binary search," in Proc. SPIE, Human Vision, Visual Proc., Digital Display III, vol. 1666, San Jose, CA, pp. 96-108, Feb. 1992.

[3] D. J. Lieberman and J. P. Allebach, "Efficient model based halftoning using direct binary search," IEEE Int. Conf. Image processing, vol. 1, pp. 755-778, 1997.

[4] S. H. Kim and J. P. Allebach, "Impact of HVS models on model-based halftoning," IEEE Trans. Image Processing, vol. 11, no. 3, pp. 258-269

[5] R. A. Ulichney, "The void-and-cluster method for dither array generation," in proc. SPIE, Human Vision Visual Processing, Digital Displays IV, vol. 1913, pp. 332-343, 1993.

[6] R. W. Floyd and L. Steinberg, "An adaptive algorithm for spatial gray scale," in Proc. SID 75 Dig.: Society for information Display, pp.36-37, 1975.

[7] D. E. Knuth, "Digital halftones by dot diffusion," ACM Trans. Graph., vol. 6, no. 4, Oct. 1987.

[8] R. Nasanen, "Visibility of halftone dot texture," IEEE Trans. Syst. Man. Cyb., vol. 14, no. 6, pp. 920-924, 1984.

[9] H. Zhang, "The optimality of naïve Bayes," Proc. 7th International Florida Artificial Intelligence Research Society Conference (FLAIRS), pp. 562-567, 2004.

[10] K. T. Knox, "Digital watermarking using stochastic screen patterns," U.S. Patent 5734752.

[11] M. S. Fu and O. C. Au, "Data hiding in halftone images by stochastic error diffusion," IEEE International Conference on Acoustics, Speech and Signal Processing, pp. 1965-1968, May 2000.

[12] S. C. Pei, J. M. Guo, H. Lee, "Novel robust watermarking technique in dithering halftone images," IEEE Signal Processing Letters, vol. 12, no. 4, pp. 333-336, April 2005.

[13] J. M. Guo, M. F. Wu, and Y. C. Kang, "Watermarking in conjugate ordered dither block truncation coding images," Signal Processing, vol. 89, no. 10, pp. 1864-1882, October 2009.

[14] J. M. Guo and Y. F. Liu, "Hiding multitone watermarks in halftone images," IEEE Multimedia, vol. 17, pp. 34-43, January 2010.
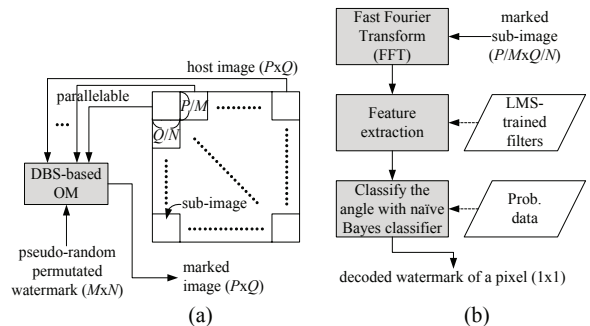
Fig. 1. Conceptual flowchart of the proposed (a) DBS-based OM encoding scheme, (b) decoding scheme.

Fig. 2. Four marked sub-images (left) and the corresponding patterns in the frequency domains (right), where the sub-images are generated by the proposed DBS-based OM and the embedded watermark is with 2-bit pixel depth, the parameter of the quality factor η is set at 2. These sub-images are marked with (a) 0°, (b) 45°, (c) 90°, and (d) 135°, respectively.
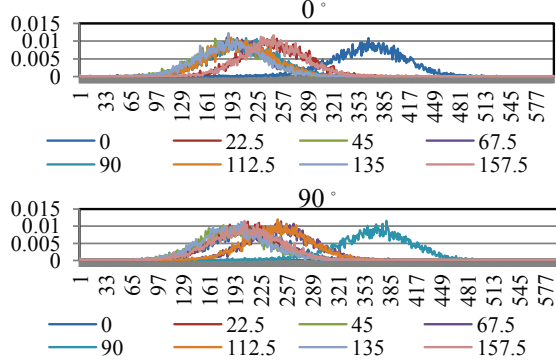

Fig. 3. Feature distributions obtained with angle 0° and 90° LMS-trained filters, each of feature distributions is constructed by 25600 halftone patterns in the frequency domain.
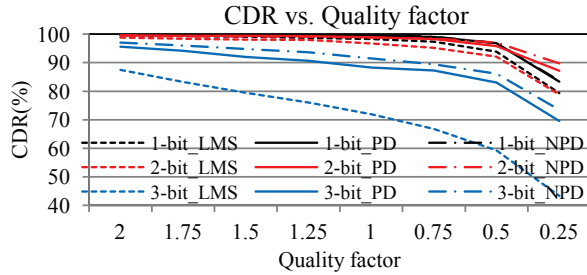
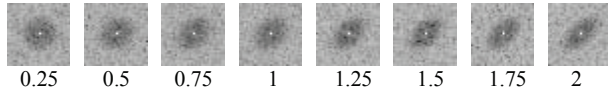Fig. 4. Averaged CDR comparisons under various numbers of bits.

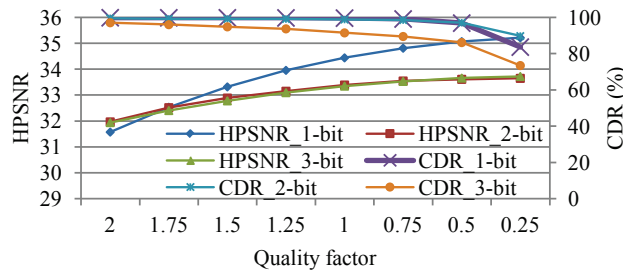Fig. 5. Eight different quality factors with identical 45°.

Fig. 6. The relationships among quality factor (η), image quality (HPSNR), and decoded rate (CDR).
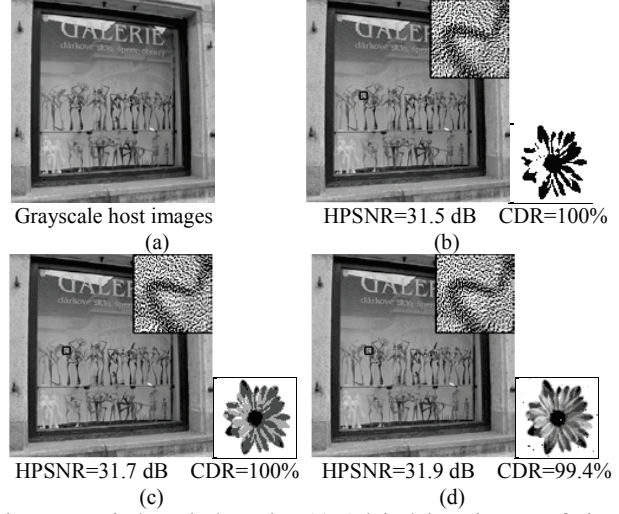

Fig. 7. Practical marked results. (a) Original host images of size 2048x2048. The marked images and the decoded watermarks with (b) 1 bit, (c) 2 bits, and (d) 3 bits, and the enlarged parts are of size 64x64. (host/marked images are printed at 600 dpi, and watermarks are printed at 72 dpi)
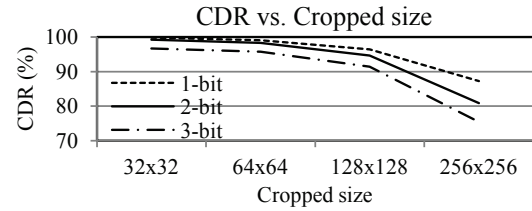

Fig. 8. CDRs under cropping attack with various cropped sizes, including 32x32 to 256x256. The size of a host image is 512x512.
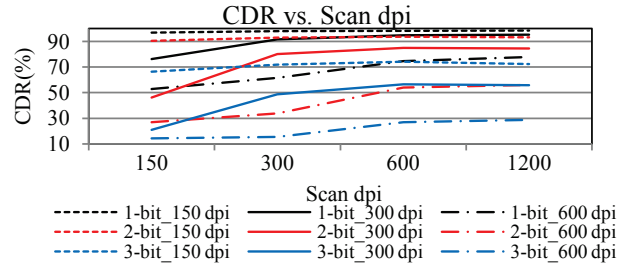

Fig. 9. Averaged CDRs of the decoded watermarks undergone print-and-scan distortion. Watermarks of various pixel-depths are adopted.

TABLE I COMPARISONS AMONG VARIOUS FORMER METHODS AND THE PROPOSED METHOD. (ADVANTAGES (+) AND SHORTCOMINGS (-))

	Image quality	Robustness	Processing efficiency	Data capacity	Additional special features
Knox [10]	-	+	+	-	Survive over print-and-scan distortion.
Fu-Au [11]	-	-	+	+	Secret sharing strategy to improve the security
Pei et al. [12]	-	+	-	+	Poor image quality
Guo et al. [13]	+	+	+	-	Low data capacity
Guo-Liu [14]	+	-	+	+	High data capacity while low robustness
Proposed method	+	+	+	+	Able to embed multi-bit watermark and overcome print-and-scan distortion. The parallelism also improves the processing speed with high quality DBS-based scheme